Letters in Applied NanoBioScience
Open-Access Journal (ISSN: 2284-6808)

Article
Volume 13, Issue 1, 2024, 12
https://doi.org/10.33263/LIANBS131.012

Adsorption and Corrosion Inhibiting Behavior of *Black Vitex Nigundo* leaf Extract on Mild Steel Corrosion on 1N HCl and 1N H_2SO_4

Subbiah Perumal [1], Shenbagapushpam Muthumanickam [2], Arumugam Elangovan [2], Nagappan Muniyappan [1], Ramaraj Sayee Kannan [2], Kommiya Krishnamoorthi [1,*]

[1] Research Center in Chemistry, Saraswathi Narayanan College, Madurai-625022, India
[2] Research Department of Chemistry, Thiagarajar College, Madurai-625009, India
* Correspondence: mothi63@yahoo.com (K.K.M.);

Scopus Author ID 6507088035
Received: 21.09.2022; Accepted: 30.10.2022; Published: 23.04.2023

Abstract: The corrosion inhibitory effect of mild steel in both 1N HCl and 1N H_2SO_4 acid media was investigated in the presence of Black *vitex nigundo* leaf (BVNL) extract as a green inhibitor. The effect of temperature, time, and inhibitor concentration was studied using the mass loss technique, electrochemical impedance spectroscopy, and potentiodynamic polarization measurement. The inhibition efficiency of Black *vitex nigundo* leaf (BVNL) extract increases with an increase in the concentration of the BVNL extract but decreases with temperature. Polarization measurements revealed that the BVNL extract acts as an anodic type inhibitor in acid media. The adsorption of BVNL extract on mild steel obeyed the Langmuir adsorption isotherm for 1N HCl, and the Freundlich adsorption isotherm was fitted for 1N H_2SO_4 media. The Maximum inhibition efficiency by the BVNL extract (90.55% in HCl and 83.14% in H_2SO_4) has been observed at a concentration of 0.075 g/l (optimum concentration) at 308 K. Surface studies such as SEM, and FT-IR was also studied to ascertain the corrosion inhibitive property of the plant extract in both acid media. Hence, BVNL extract acts as an eco-friendly and efficient green corrosion inhibitor for mild steel in 1N HCl and 1N H_2SO_4 acid media.

Keywords: BVNL extract; green inhibitors; potentiodynamic polarization; EIS; SEM.

© 2023 by the authors. This article is an open-access article distributed under the terms and conditions of the Creative Commons Attribution (CC BY) license (https://creativecommons.org/licenses/by/4.0/).

1. Introduction

Metals and their alloys are exposed to the action of acids in industry. In an acid medium, the corrosion rate of metallic materials can be readily reduced by using corrosion inhibitors [1]. Due to its toxic nature and the high cost of synthetic chemicals currently in use, developing environmentally suitable and less expensive chemicals as corrosion inhibitors is essential. Natural inhibitors can be considered as best alternatives for this purpose [2] as their phytoconstituents have been found to be effective as the best alternatives for this purpose [2] as their phytoconstituents have been found to be effective corrosion inhibitors in acid media. It has been found that the corrosion inhibitors having O, N, or S atoms in their structures donate electrons for bonding with the metal surface.

However, current research deals with effective and reliable corrosion inhibitors from pharmaceutical drugs and plant extracts as organic green corrosion inhibitors. Moreover, natural products of plant origin containing different organic compounds like alkaloids, tannins, flavonoids, pigments, organic amino acids, etc., are known to have inhibitive action [3,4].

Corrosion of metal is a major crisis that has affected the world for centuries. As an economical technique for protecting metals against corrosion, corrosion inhibitors remain the most effective, simplest, and most applied solution. Corrosion is basically an electrochemical process [5-8].

During corrosion, iron atoms undergo oxidation and prevent a further anodic reaction, or corrosion [9]. Since the corrosion current also flows through the electrolyte by ionic conduction, this will influence how corrosion cells operate. The corroding piece of metal can act as a mixed electrode since both anodic and cathodic reactions are taking place on its surface [10].

Metals are a valuable resource for a country. Most metals, such as iron, aluminum, copper, chromium, manganese, titanium, etc., are declining fast, leading to an acute shortage of these valuable metals. An impending metal crisis does not seem anywhere to be a remote possibility but a reality [11,12]. Corrosion has been a very important factor contributing to disasters. The awareness of corrosion inhibition can minimize such disasters [13-16]. The replacement of some expensive chemicals as corrosion inhibitors for the metal in acid-cleaning processes with naturally occurring substances of plant origin has been thoroughly studied [3, 17-19].

The usage of biological products in corrosion inhibition of steel in an acidic medium (HCl, H_2SO_4) has been established by many research studies [3, 20,21].

Saleh reported that Opuntia ficus indicia extracts, Aloe leaves, and orange, mango, and pomegranate peels could protect steel in 5% and 10% HCl at 25^o C and 400^{o}C. Srivastava found that tobacco, black pepper, castor oil seeds, acacia gum, and lignin could be good corrosion inhibitors for steel in an acidic medium [22-26].

Recently, Pharmacognostic studies on methanolic Extract of Leaves of *Vitex negundo Linn* have been reported [27]*Black vitex nigundo* belongs to the plant family called Verbenaceae, and in Tamil, it is called Karunochi leaves or Nirgundi. Plant materials generally contain proteins, polysaccharides, polycarboxylic acids, and alkaloids.

BlackVitex negundo leaves are astringent, sedative, tonic, and vermifuge. It is useful in dispersing swellings of the joints from acute rheumatism. It is also used to repel insects in grain stores. Extract of the leaves has insecticidal efficiency. The fresh leaves are burnt with grass as a fumigant against mosquitoes [28]. Very few studies have been reported on corrosion inhibition studies of *Black vitex nigundo* plant extract. This prompted us to study the corrosion-inhibiting behavior of *Black vitex nigundo* leaf extract on mild steel corrosion. The present study has investigated the corrosion inhibitory effect of the ethanol extract of the *Black Vitex negundo* leaf on metal in 1N HCl and 1N H_2SO_4 media.

2. Materials and Methods

2.1. Preparation of the specimens.

Earlier to all dimensions, the mild steel samples have been polished with different emery papers up to 4/0 grades, and mild steel specimen composition has stood as C: 0.13, Si: 0.18, P: 0.39, S: 0.04, Cu: 0.025 and the balance Fe. The specimen of mild steel has been mechanically cut to form different coupons, each measuring exactly 2.5 × 2.5 × 0.4 cm. Each specimen has been degreased by washing with acetone, then dried at room temperature and preserved in desiccators. All reagents for the present learn have been Analar grade, and distilled water has been used for their preparation.

2.2.Preparation of leaves extract.

Black Vitex negundo leaves have been used to make ethanol extract. BVNL were collected in and around Madurai, Tamil Nadu, and India; the leaves were dried, grained, and soaked in distilled water for 6 hrs. After 6 hrs, the crude extract has been boiled, cooled, and triple-filtered. The extract of *Black Vitex negundo* leaf obtained in this manner can be used as an inhibitor.

2.3.Preparation of test solution.

The concentration solution (1N HCl and 1N H_2SO_4) was prepared by diluting Analytical Grade 98% H_2SO_4 and HCl with double-distilled water. The solution volume has stood at 100ml with and without the addition of various concentrations of *Black Vitex negundo* extract.

2.4. Weight loss method.

Weight loss measurements for each lope have been placed in a glass vessel containing 100 mL of test solution. A sanitary mild steel square specimen has been entirely placed immersed in 100 mL of inhibitor solution and blank solutions in a thermostatted water bath. The temperature of the solution has been maintained in the range of 308—333 K. After 2 hrs immersion. The specimens were taken from the solution, rinsed with double distilled water, systematically dehydrated, and weighed. The corrosion rate (CR) and the inhibition efficiency (IE) are calculated from the weight loss (ΔW).

$$\text{corrosion rate(mpy)} = \frac{\text{KW}}{\text{DAT}}$$

K= 534 to give CR in mpy and K= 87.6 to give CR in mm/yr

Where D is the density of the specimen (g/cm^3), A is the area of the specimen in inch^2 and T is the period of immersion in hours, W= weight loss (W_b-W_a), where Wb and W_a are the specimen weights before and after immersion in the tested solution.

$$\text{Corrosion rate(mpy)} = \frac{534\ \text{X wt loss}_{(g)}(W_b - W_a)}{\text{Density(D)X Area(inch)X Time(h)}} \quad (1)$$

$$\text{IE \%} = [(W_0 - W_1)/W_0] \times 100 \quad (2)$$

The CR is expressed in terms of either mils (1/1000 inch) per year (mpy) or millimeters per year (mm/yr).The k value is constant, and its magnitude depends on the system of units used. W_0 and W_1 are the weight loss of mild steel in the absence and presence of an inhibitor, respectively.

2.5. Electrochemical measurements.

Polarization curves and impedance curves have been drawn and recorded using CHI electrochemical workplace impedance analyzer model CHI 604D. The working polished mild steel electrode with an exposed area of 0.5 cm^2 has been placed and immersed in a test solution. A cell containing three compartments for electrodes has been used. A platinum and a saturated calomel electrodes have been used as the counter and reference electrodes. Before electrochemical experiments, the electrode was allowed to rust freely, and its open-circuit potential was recorded. Potentiodynamic polarization curves have stood recorded from -300 to +300 m Vsce, (verses OCP) with a scan rate of 1 Vs^{-1}. Electrochemical impedance spectroscopy measurements have been performed using the frequency range of 0.1 Hz to 100

K Hz. All measurements have been studied at 308 K using 100 ml of electrolyte (1 N HCl and 1N H_2SO_4) in a stationary condition. Every experiment has been repeated in triplicate to check the reproducibility of the data.

2.6. Surface analysis studies.

2.6.1. Fourier Transform Infra-Red spectroscopy.

FT-IR has been recorded in the SHIMADZU-FTIR-8400S spectrophotometer. For FT-IR characterization, the mild steel stood immersed for 2 hrs in 100 ml 1 N HCl and 1N H_2SO_4 solution containing 600 ppm *Black Vitex Negundo*leaf extract. After 2 h, the specimens were taken out, dried, rubbed with a small amount of KBr powder, and made into a disk.

2.6.2. SEM analysis.

The mild steel specimens have been placed and immersed in acid solutions in the absence and presence of the most favorable concentration of inhibitor for a period of 2 hrs. After 2 hrs, the specimens were taken out and dried. The character of the surface film formed on the mild steel specimen has been examined with a JEOL (JSM 6390) Scanning Electron Microscope and Scanning Probe Microscope (Akilan Technology UK 5500 series).

3. Results and Discussion

3.1. Weight loss measurements.

The efficiency of inhibition (%) and rate of corrosion (CR) obtained from the measurement of weight loss for different concentrations of BVNLE on mild steel in 1N HCl and 1N H_2SO_4 at 308 - 333 K are given in Table 1 and show that the percentage inhibition increases with increasing concentration of BVNLE [29]. This indicates that the surface coverage of metal by adsorption of BVNLE increases with increasing concentration of plant extract. Maximum inhibition efficiency by the BVNLE (90.55% in 1N HCl and 83.14% in 1N H_2SO_4) is observed at a concentration of 750ppm (optimum concentration of plant extract) at 308 K. A further increase of inhibitor concentration does not change the inhibition efficiency significantly.
Temperature is an important condition in studies of metal dissolution. An increase in temperature may affect the metal surface, for example, rapid etching, inhibitor desorption, and inhibitor decomposition. Hence, the inhibition properties of BVNLE are also discussed on the basis of a kinetic model.

Table 1. Corrosion rate and inhibition efficiency of mild steel specimens immersed in 1N HCl and 1N $H_2SO_4$with and without BVNLE at different temperatures

Test Solution	Temperature (K)	Concentration (ppm)	Corrosion Rate (mpy)	Surface coverage(Θ)	Inhibition Efficiency (%)
1N HCl	308	0	0.180		
		600	0.025	0.8611	86.11
		650	0.022	0.8770	87.70
		700	0.020	0.8888	88.88
		750	0.017	0.9055	90.55
	313	0	0.429		
		600	0.078	0.8181	81.81
		650	0.073	0.8298	82.98
		700	0.068	0.8414	84.14
		750	0.052	0.8787	87.87
	323	0	0.662		

Test Solution	Temperature (K)	Concentration (ppm)	Corrosion Rate (mpy)	Surface coverage(Θ)	Inhibition Efficiency (%)
		600	0.136	0.7945	79.45
		650	0.126	0.8096	80.96
		700	0.120	0.8187	81.87
		750	0.090	0.8549	85.49
		0	1.058		
	333	600	0.265	0.7484	74.84
		650	0.245	0.7684	76.84
		700	0.220	0.7920	79.20
		750	0.200	0.8109	81.09
		0	0.458		
	308	600	0.091	0.8013	80.13
		650	0.087	0.8100	81.00
		700	0.079	0.8275	82.75
		750	0.074	0.8314	83.14
		0	1.009		
	313	600	0.248	0.7542	75.42
		650	0.220	0.7819	78.19
		700	0.213	0.7888	78.88
1N H_2SO_4		750	0.193	0.8087	80.87
		0	1.870		
	323	600	1.033	0.4475	44.75
		650	0.859	0.5406	54.06
		700	0.698	0.6267	62.67
		750	0.638	0.6588	65.88
		0	2.418		
	333	600	1.532	0.3664	36.64
		650	1.399	0.4214	42.14
		700	1.127	0.5339	53.39
		750	0.991	0.5900	59.00

The corrosion rate of mild steel in 1N HCl and 1N H_2SO_4in the absence and presence of different concentrations of BVNLE was determined at 308 - 333 K. The inhibition efficiency of BVNLE on mild steel in 1N HCl and 1N H_2SO_4 at different temperatures is investigated. The maximum inhibition efficiency was found to be 90.55% and 83.14 at 308 K, indicating that BVNLE was a good corrosion inhibitor in an acid medium. The plots of corrosion rate with temperature for various concentrations of inhibitor in 1N HCl and 1N H_2SO_4 media are shown in Figure 1.

Figure 1 shows that the inhibition efficiency decreased with the increase in temperature. The higher inhibition efficiency of the BVNLE was observed at 308 K.

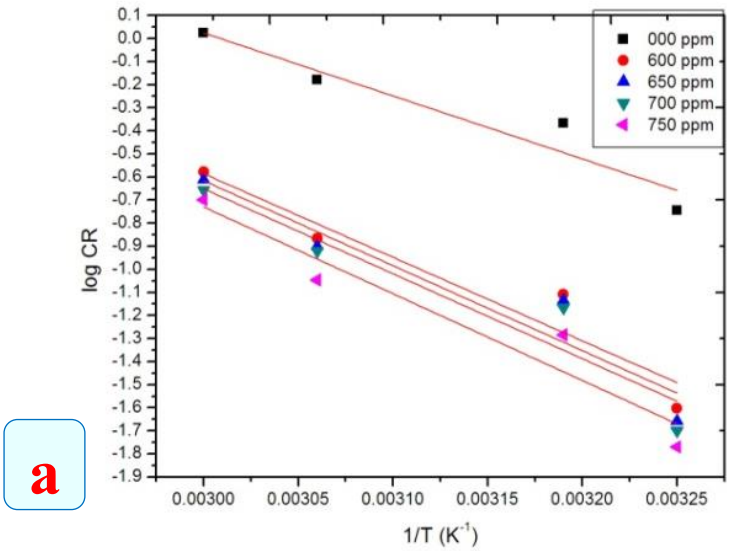

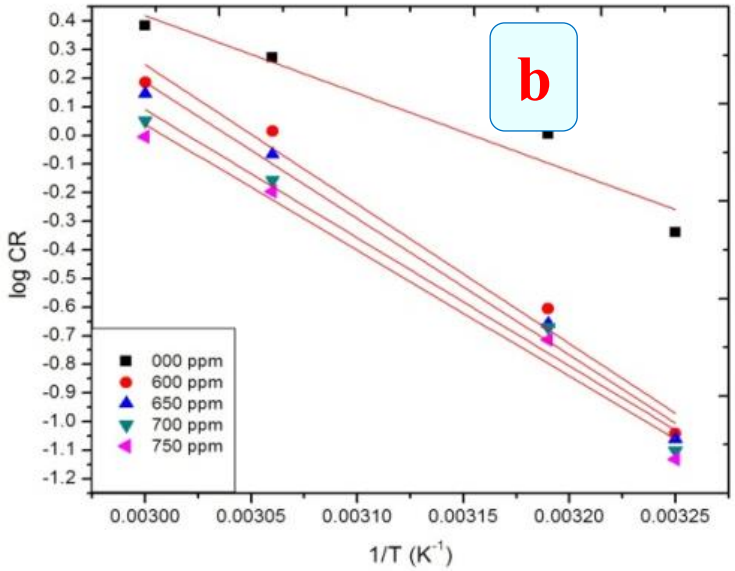

Figure 1. Arrhenius plot of log CR versus 1/T at different concentrations of BVNLE in **a)** 1N HCl and **b)**1N H_2SO_4

3.2. Thermodynamic studies.

The activation parameters, mainly the activation energy (E_a), the enthalpy of activation (ΔH), and the entropy of activation (ΔS) were calculated from the Arrhenius equation

$$CR = A \exp(-E_a/RT) \quad (3)$$

Taking the logarithm of both sides of the above equation could be obtained

$$\log CR = \log A - E_a/2.303\ RT \quad (4)$$

The transition state equation estimated the change of enthalpy (ΔH) and entropy (ΔS) for the formation of the activated complex in the transition state.

$$\log CR/\ T = \{ (\log R/hN + (\Delta S)/2.303\ R)\} - \Delta H/2.303\ RT \quad (5)$$

where CR is the corrosion rate, A is the pre-exponential factor, h is Planck's constant, N is Avogadro's number, E_a is the apparent activation energy, R is the gas constant (R= 8.314 J mol^{-1} K^{-1}), and T is the absolute temperature.

Figure 3.1 shows the Arrhenius plot, and the slope of the straight line is equal to -E_a/2.303 R and the intercept is equal to log A. The obtained values of E_a were determined in solutions containing extracts of BVNLE could be interpreted as physisorption. The activation energy values are increased by the addition of BVNLE to the acidic blank solution. A plot of log CR/T vs. 1/T(Figure 2) gave a straight line with a slope of the line (-ΔH/2.303R) and an intercept (log R/hN +(ΔS)/2.303 R) from which the values of ΔH and ΔS were calculated and summarized in Table 2.

Table 2. Corrosion kinetic parameters for mild steel in 1N HCl and 1N H_2SO_4 in the absence and presence of different concentrations of BVNLE.

Test solution	Concentration (ppm)	E_a (kJ/mol)	-ΔH (kJ/mol)	-ΔS (J/mol/K)
1N HCl	0	52.27	167.70	197.07
	600	69.37	239.14	196.90
	650	70.52	239.14	196.90
	700	70.43	245.08	196.88
	750	71.99	251.21	196.86
1N H_2SO_4	0	-51.95	157.38	197.32
	600	-88.50	274.19	197.53
	650	-91.26	288.54	197.52

Test solution	Concentration (ppm)	E_a (kJ/mol)	-ΔH (kJ/mol)	-ΔS (J/mol/K)
	700	-85.74	270.16	197.55
	750	-84.21	266.52	197.59

These data found that the thermodynamic parameters, ΔH and ΔS, of the dissolution reaction of mild steel in 1N HCl and 1N H_2SO_4 in the presence of BVNLE were higher than the uninhibited solution. The negative signs of the enthalpies ΔH reflected the exothermic nature of the steel dissolution process. The negative values of ΔS indicate that a decrease in disorders took place on going from reactants to the activated complex. This result obeys the work by Olatunde Alaba Akinbulumoa *et al*. [30].

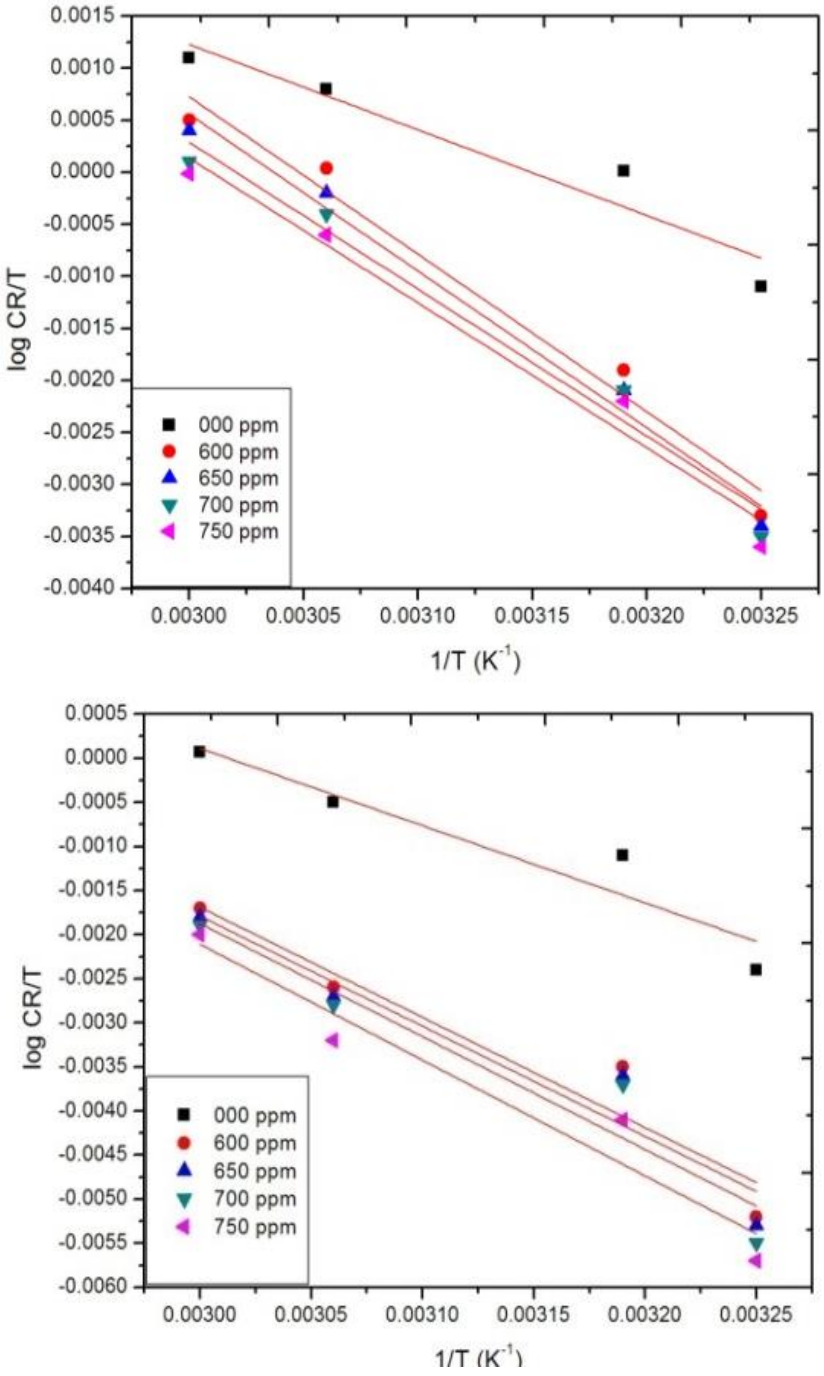

Figure 2. Transition state plots log CR/T versus 1/T at different concentrations of BVNLE in **(a)** 1N HCl and **(b)** 1N H_2SO_4.

3.3. Adsorption isotherm.

The essential information on the adsorption of the inhibitor on the metal surface can be obtained from the adsorption isotherm. The θ values of different concentrations of inhibitor were tested by fitting to various isotherms, including Frumkin, Langmuir, Temkin, and Freundlich isotherms. In this study, the results fitted best the Langmuir adsorption isotherm for 1N HCl, and the Freundlich adsorption isotherm was fitted for 1N H_2SO_4, which is given by,

$$C/\theta = 1/K_{ads} + C \quad (6)$$

where K_{ads} is the equilibrium constant of the adsorption process, C is the concentration inhibitor, and θ is the surface coverage. In 1N HCl, the best-fitted straight line was obtained for the plot of Cvs.C/θ with a slope of almost unity (Figure 3a). In 1N H_2SO_4 medium, a best-fitted straight line was obtained for the plot of log C vs.C/θ Figure 3(b) This behavior indicated that the adsorption of BVNLE on mild steel surface obeyed the Langmuir adsorption isotherm in 1N HCl and Freundlich adsorption in 1N H_2SO_4.

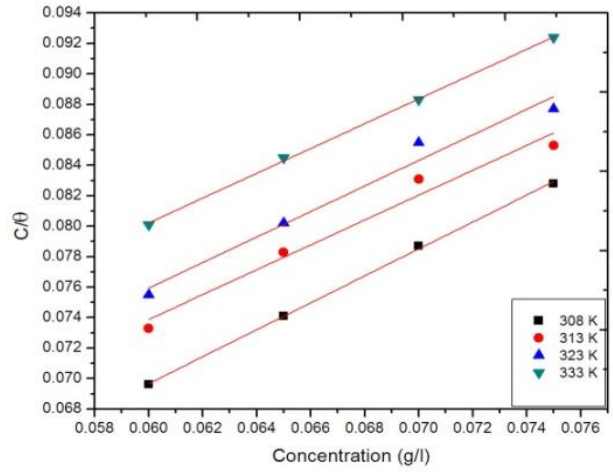

(a)

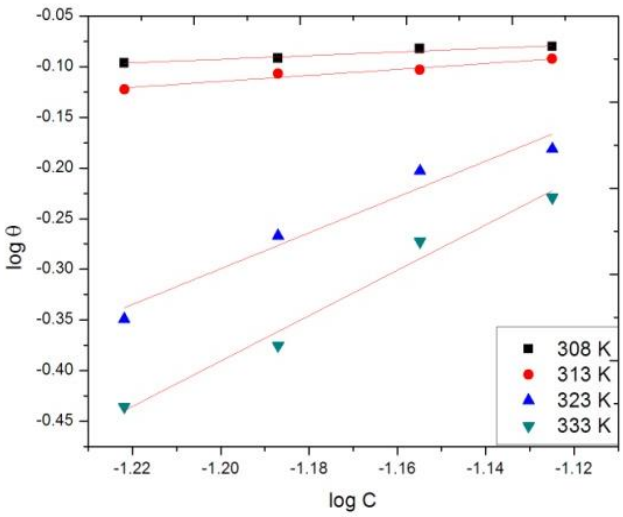

(b)

Figure 3. **(a)** Langmuir adsorption isotherm for mild steel in 1N HCl containing different concentrations of BVNLE at different temperatures; **(b)** Freundlich adsorption isotherm for mild steel in 1N H_2SO_4 containing different concentrations of BVNLE at different temperatures.

The free energy values of adsorption (ΔG_{ads}) of BVNLE on mild steel surfaces were calculated using the following equation (6).

$$\Delta G_{ads} = - RT \ln (55.5 K_{ads}) \quad (7)$$

where R is the gas constant, T is the absolute temperature, and 55.5 is the molarity of water in the solution. The values of K_{ads} were found to decrease with increasing temperature in both acids media showing the adsorbed molecules are weakly adsorbed on the metal surface. In the present study, the negative value of ΔG_{ads} (Table 3) indicated the spontaneous adsorption of BVNLE on a mild steel surface and strong interactions between inhibitor molecules and the metal surface. Generally, the values of ΔG_{ads} up to -20 kJ/mol signifies physisorption [31], which is consistent with electrostatic interaction between charged molecules and a charged metal. In our system, the calculated values of ΔG_{ads} were around -20 kJ/mol, indicating that the adsorption of the BVNLE on mild steel in both 1N HCl and 1N H_2SO_4 solutions at the studied temperatures was physisorption in nature.

Table 3. a) Langmuir adsorption parameters and free energy of adsorption ofBVNLE as an inhibitor on the surface of mild steel in 1N HCl .b) Freundluchadsorption parameters and free energy of adsorption ofBVNLE as an inhibitor on the surface of mild steel in 1N H_2SO_4

Test solution	Temperature (K)	$-\Delta G^0_{ads}$ (kJ/mol)	$K_{(ads)}$	R^2 value
1N HCl	308	20.87	62.50	0.999
	313	20.16	41.60	0.973
	323	20.69	40.00	0.975
	333	20.74	32.20	0.999
1N H_2SO_4	308	15.66	08.19	0.954
	313	14.18	04.20	0.958
	323	09.13	00.54	0.972
	333	08.78	00.43	0.977

3.4. Electrochemical studies.

3.4.1.Potentiodynamic polarization measurements.

The potentiodynamic polarization curves of mild steel immersed in the absence and presence of inhibitors in 1N HCl and 1N H_2SO_4 are shown in Figure 4.

The corrosion parameters, namely corrosion potential (E_{corr}), corrosion current (I_{corr}), cathodic slope (β_c), anodic slope (β_a), Linear polarization resistance (LPR), and percentage of inhibition efficiency calculated from Tafel plots, are given in Table 4.

Table 4. Potentiodynamic polarization parameters for the corrosion of mild steel in 1N HCl and 1N H_2SO_4 containing different concentrations of BVNLE.

Test solution	Concentration(ppm)	E_{corr}(mV)	I_{corr} (µA cm^{-2})	β_c (mV/decade)	β_a (mV/decade)	R_p (ohm cm^2)	IE %
1N HCl	0	-458	341.7	188.92	149.92	11	-
	600	-458	54.28	182.54	87.07	46	84.11
	650	-458	55.3	179.53	83.20	46	83.81
	700	-466	36.6	171.76	74.00	61	89.28
	750	-485	29.9	165.12	86.39	82	91.24
1N H_2SO_4	0	-449	5976	204.20	142.10	6	-
	600	-444	3034	220.02	137.64	12	49.23
	650	-442	2348	219.01	136.20	16	60.70
	700	-443	2182	216.40	139.27	17	63.48
	750	-441	1496	189.17	124.33	22	74.96

The inhibition efficiency is defined as,IE % = (i^0_{corr} - i_{corr}/i^0_{corr}) × 100 (6)
where i^0_{corr} and i_{corr} are the corrosion current density values without and with inhibitor, respectively.

The change in values of both $\beta_a$and β_c suggested that the reaction is an anodic and cathodic controlled one, and the BVNLE acts as a mixed-type inhibitor [32,33]. Moreover, in the presence of the inhibitor system, the corrosion current decreased from 341.7 to 29.31 µA/cm^2 in 1N HCl and also decreased from 5976 to 1496 µA/cm^2 in 1N H_2SO_4, and LPR values increased from 11 to 82 ohm cm^2 in 1N HCl and 6 to 22 ohm cm^2 in 1N H_2SO_4. These observations confirmed that BVNLE is a good inhibitor in both acid media [34].

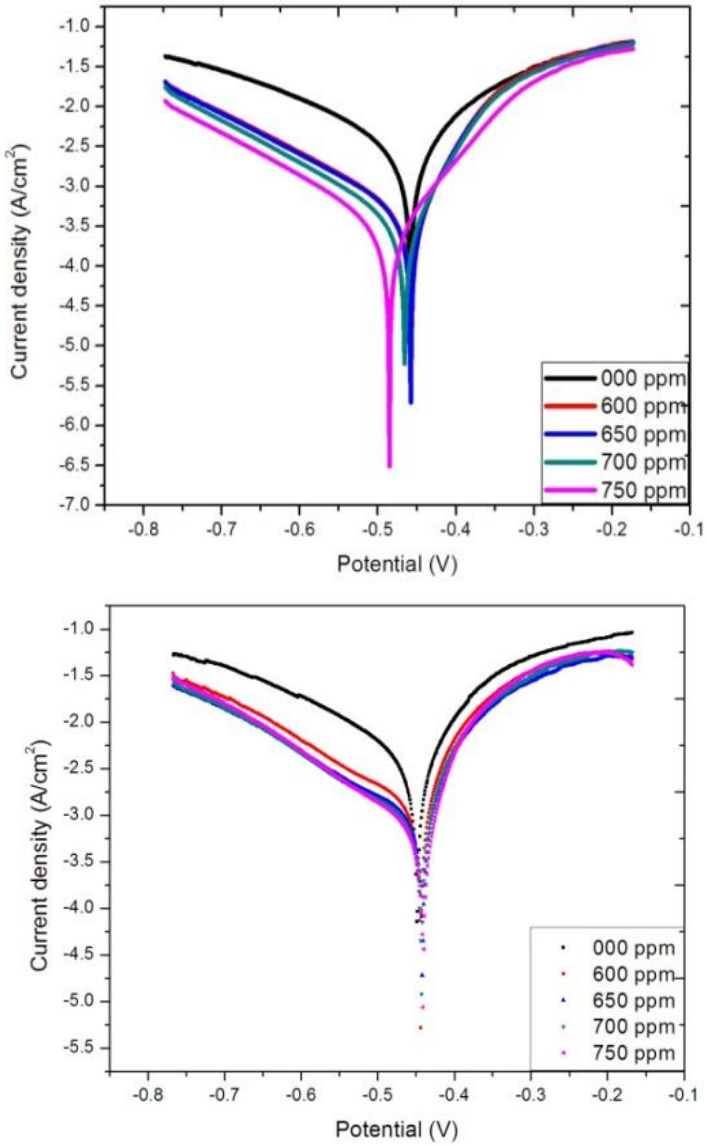

Figure 4. Tafel plots of mild steel immersed in (**a**)1N HCl and (**b**) 1N H_2SO_4 with and without BVNLE.

3.4.2. Electrochemical impedance measurements.

Impedance spectra obtained for mild steel in 1N HCl and 1N H_2SO_4 in the presence and absence of the inhibitors are shown in Figure 5. The impedance parameters such as R_s, R_{ct}, and C_{dl} derived from Nyquist plots are given in Table 5.

The charge transfer resistance (R_{ct}) increased with an increase in the concentration of inhibitor in the acid solution. In the impedance studies, IE % was calculated as:

$$IE\ \% = (R_{ct(inh)}\text{-}R_{ct}/R_{ct(inh)}) \times 100 \quad (7)$$

where R_{ct} and $R_{ct(inh)}$ are uninhibited and inhibited charge transfer resistance, respectively, the diameter of Nyquist plots increased the concentration of BVNLE in both acid media, indicating the strengthening of the inhibitor film. In both acid media, the concentration of the inhibitor increased, charge transfer resistance enhanced and decreased the double-layer capacitance values, and the double-layer capacitance values decreased [35].

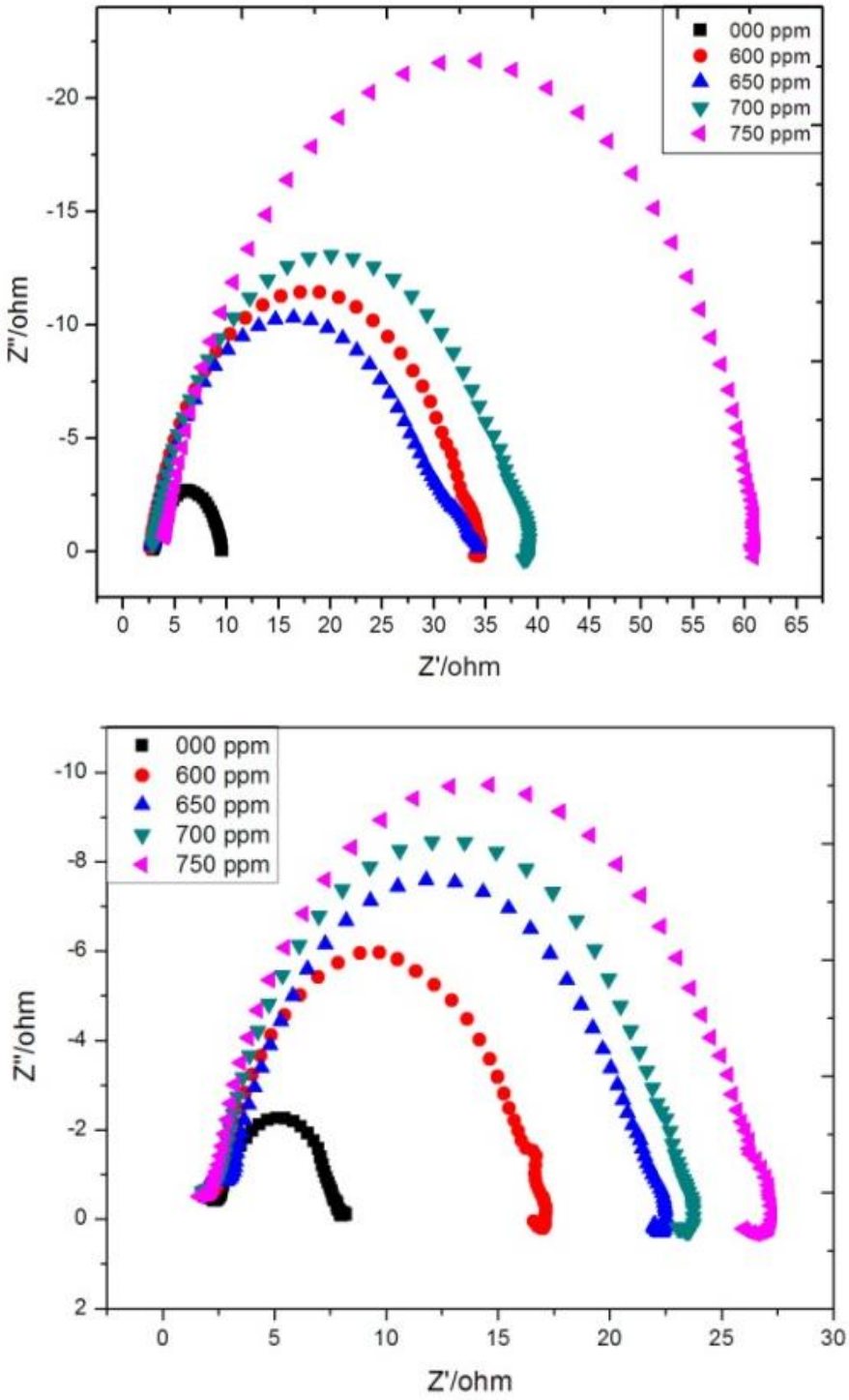

Figure 5. Nyquist plots for mild steel immersed in (**a)** 1M HCl and (**b)** 1N H_2SO_4different concentrations of BVNLE at 308 K.

It is due to the adsorption of BVNLE on the metal surface leading to the formation of the protective layer on the electrode surface [36] and decreasing the extent of the dissolution

reaction. These results are good experimental proof for inhibiting BVNLE on mild steel in 1N HCl and 1N H_2SO_4.

Table 5. Electrochemical impedance parameters for mild steel in 1N HCl and 1N H_2SO_4 in the absence and presence of BVNLE.

Test solution	Concentration (ppm)	R_s (Ω cm^{-2})	R_{ct} (Ω cm^{-2})	C_{dl} (F/cm^2)	IE %
1N HCl	0	2.795	6.968	8.5×10^{-3}	--
	600	0.973	34.956	4.0×10^{-4}	80.06
	650	0.238	36.537	1.1×10^{-5}	80.92
	700	0.786	40.194	3.0×10^{-4}	82.66
	750	1.441	61.907	1.2×10^{-4}	88.71
1N H_2SO_4	0	2.139	05.902	1.1×10^{-2}	--
	600	1.706	15.665	1.7×10^{-3}	62.32
	650	2.018	20.891	9.9×10^{-4}	71.74
	700	1.445	22.901	8.2×10^{-4}	74.22
	750	0.865	28.267	5.9×10^{-4}	79.12

3.5.FT-IR spectral studies.

FT-IR spectroscopy is used to predict the type of bonding between organic inhibitors and the metal surface. The FT-IR spectra of the BVNLE and its resulting solutions after mild steel immersion in both media are shown in Figures 6 a and b.

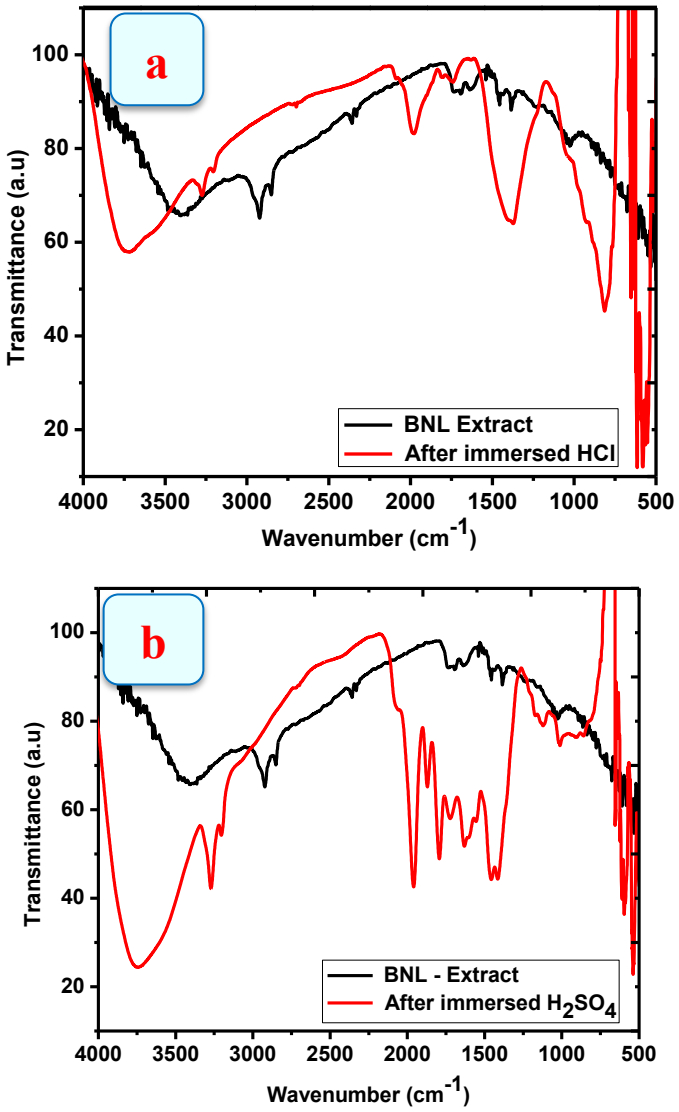

Figure 6 FT-IR Spectra for BVNLE **(a)** BVNLE and after immersion 1N HCl and**(b)** BVNLE and after immersion 1N H_2SO_4.

A broad peak is obtained at 3381 cm^{-1}corresponds to N-H / O-H stretching vibration. The frequency at 2930 cm^{-1} is assigned to the C-H stretching frequency. The absorption of a strong peak at 1617 cm^{-1} corresponds to C=C or C=N stretching or N-H bending vibrations. The absorption band at 1468 cm^{-1}assigned to C-H bending in $–CH_3$ or O-H bending vibrations. Peaks at 1030 cm^{-1} and 1370 cm^{-1} are observed due to C-N and C-O stretching vibrations. On the basis of the results, BNVLE has (N-H, N=C=S, C=N, C-N, OH, C=O, C-O) various functional groups and aromatic rings, which make the extract as the inhibitor in the mild corrosion steel. The N–H stretching, shifted from 3381 to 3735 cm^{-1}, indicates the coordination of inhibitor with Fe^{2+} through the N atom of the N–H group in both media. The shifting of C=C stretching from 1617 to 1980 cm^{-1} might confirm a strong interaction between BNVLE and the mild steel surface.

3.6.Morphological studies.

The SEM images of the mild steel surface after immersion in 1N HCl and 1N H_2SO_4 in the presence of BVNLE for 2 hours are shown in Figure 7. After 2 hours, the specimens were taken out and dried. SEM images showed that the surface of the inhibited sample of mild steel specimens was better than the uninhibited sample [37]. This examination indicated that the corrosion rate was reduced in the presence of inhibitors. This might be due to the adsorption of inhibitor molecules on the metal surface as a protective layer.

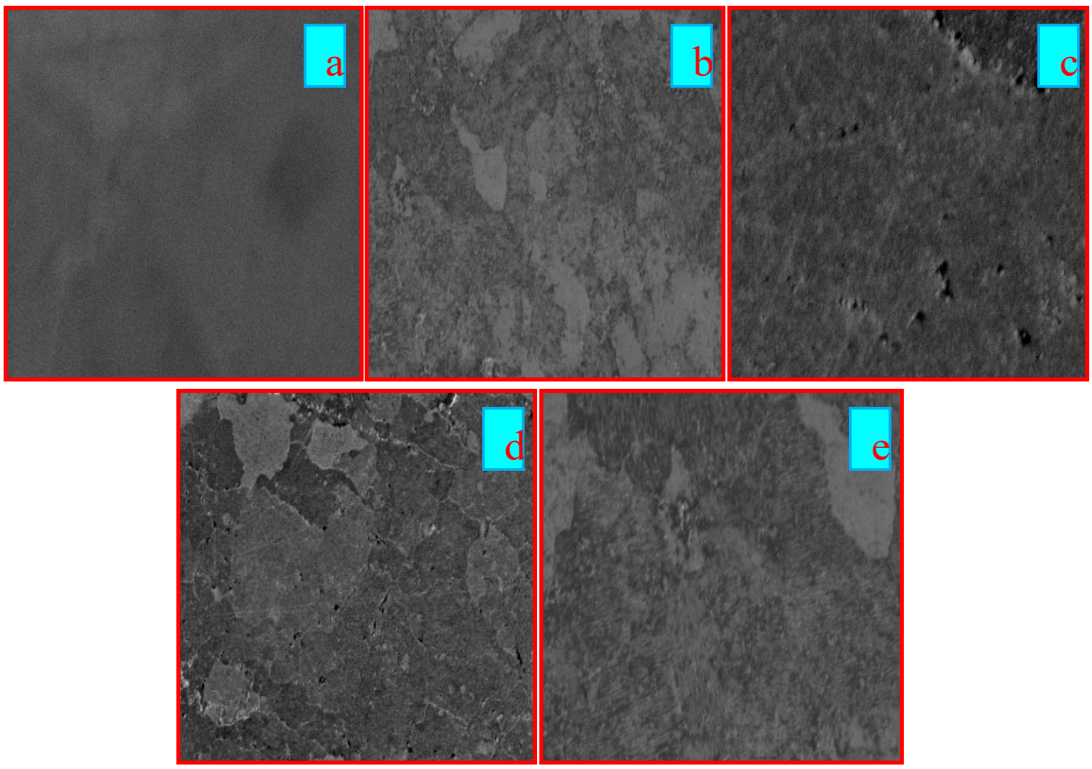

Figure 7.SEM images of **(a)** plain mild steel **(b)** after immersion of 1NHCl in the absence of BVNLE **(c)**after immersion of 1N HClinthepresence of BVNLE after immersion of 1N H_2SO_4in the absence of BVNLE **(e)**after immersion of 1N H_2SO_4in the presence of BVNLE.

4. Conclusions

The ethanolic extract of BVNLE was applied as a green corrosion inhibitor on the corrosion of mild steel in 1N HCl and 1N H_2SO_4. The inhibitory effect of BVNLE for mild steel corrosion in 1N HCl and 1N H_2SO_4.solution was examined using EIS, SEM,

potentiodynamic polarization, and weight loss methods. The inhibition efficiency of mild steel in both acid media increased with the concentration of BVNLE but decreased with increasing temperature. Potentiodynamic polarization measurements revealed that BVNLE acted as a mixed-type inhibitor in both acid media. EIS measurement revealed that charge transfer increased with an increase in the concentration of BVNLE, indicating that the inhibition increased with an increase in concentrations. The adsorption of the inhibitor obeyed the Langmuir and Freundlich adsorption isotherms in 1N HCl and 1N H_2SO_4, respectively, at all investigated temperatures. The adsorption was spontaneous, and the inhibition of corrosion by BVNLE was due to the formation of physisorption on the mild steel surface. Protective film formation against acid attack was confirmed by SEM techniques. The results obtained from weight loss, polarization, and impedance measurements agree.

Funding

This research received no external funding.

Acknowledgments

One of the authors (S. Perumal) thanks UGC, New Delhi, for granting the Teacher Fellowship (FDP) and the Management of Saraswathi Narayanan College, Madurai, India, for encouragement to carry out this work. The authors are thankful to the Head, PG, and Research Department of Chemistry, Thiagarajar College, Madurai, India, for providing instrumental facilities.

Conflicts of Interest

No potential conflict of interest was reported by the authors.

References

1. Bockris, J.O.M.;& Reddy, A.K.N. Modern Electrochemistry. New York, Plenum Express. **1977.**
2. Samar. Al-Nami. Y.Corrosion Inhibition of Low Carbon Steel in 1 M HCl Solution by Cephalexin Monohydrate Drug and Synergistic Iodide Additives.**2021**, *11*,8550 – 8563,https://doi.org/10.33263/BRIAC111.85508563.
3. Popoola, L. T. Progress on pharmaceutical drugs, plant extracts and ionic liquids as corrosion inhibitors, Heliyon, **2019**, *5*, 1143-1148,https://doi.org/10.1016/j.heliyon.2019.e01143.
4. Divya, P.; Subhashini, S.; Prithiba, A.;& Rajalakshmi, R. Tithonia Diversifolia flower Extract as green Corrosion Inhibitor for Mild Steel in Acid Medium.*Materials Today Proceedings***2019**, *18*,1581-1591,https://doi.org/10.1016/j.matpr.2019.05.252.
5. Reyes-Riverol. R.;Lieblich. M.;Fajardo, S.Corrosion resistance and anomalous hydrogen evolution in chloride containing solutions of extruded cast and powder metallurgical Mg-1Zn alloy.*Corrosion Science***2022**, *208*, 110635,https://doi.org/10.1016/j.corsci.2022.110635.
6. Kusnierczyk, K.; Basista, M. Recent advances in research on magnesium alloys and magnesium-calcium phosphate composites as biodegradable implant materials. *J Biomater Appl*.**2016,** *31*, 878–900,https://doi.org/10.1177/0885328216657271.
7. Chen, J.; Song, Y.; Shan, D.;*et al*. Modifications of the hydrotalcite film on AZ31 Mg alloy by phytic acid: The effects on morphology, composition and corrosion resistance. *Corros Sci*. **2013**, 74, 130–138, https://doi.org/10.1016/j.corsci.2013.04.034
8. Shi, Z.; Liu,M.; Atrens, A. Measurement of the corrosion rate of magnesium alloys using Tafel extrapolation. *Corr Sci***. 2010**, *52*, 579–588, https://doi.org/10.1016/j.corsci.2009.10.016.

9. Zhou, X.; Xiong, W.; Zeng. G. Combined effects of LPSO orientation and α-Mg texture on tensile anisotropy of an extruded Mg-Gd-Y-Zn-Zr alloy. *Mater Sci Eng A-Struct.* **2021**, *805*, 140596, https://doi.org/10.1016/j.msea.2020.140596.
10. Wang, W.L.; He, L.; Yang, X. Research on the formation process of selective laser melting Mg–Y–Sm–Zn–Zr alloy. *Mater Sci Technol*. **2021**, *37*, 174–181, https://doi.org/10.1080/02670836.2021.1874122.
11. Jian, S.Y.; Chu, Y.R.; Lin, C.S. Permanganate conversion coating on AZ31 magnesium alloys with enhanced corrosion resistance. *Corr Sci*. **2015**, *93*, 301–309,https://doi.org/10.1016/jcorsci.2018.01.040
12. Melchers, R.E. Long-term corrosion of steels in deep, cold, low oxygen sea waters. *Corros Eng Sci Technol*. **2021**, *56*, 736–741,https://doi.org/10.1080/1478422X.2021.1954137.
13. Eldredge, G.G.;&Warner, J.C. The Corrosion Hand Book. New York., John Wiley and Sons. **1950**.
14. Czerwinski, F. Current trends in automotive lightweighting strategies and materials. *Materials* **2021**, *14*, 6631, https://doi.org/10.3390/MA14216631.
15. Sato, F.E.K.; Nakata, T. Analysis of the impact of vehicle lightweighting on recycling benefits considering life cycle energy reductions. *Resour Conserv Recycl.***2021**, *164*, 105118,https://doi.org/10.1016/J.RESCONREC.2020.105118.
16. Ashraf, S.; Naveed, M.; Afzal, M.; Ashraf, S.; Rehman, K.; Hussain, A.;& AhmadZahir , Z. Bioremediation of tannery effluent by Cr- and salt-tolerant bacterial strains. *Environmental Monitoring and Assessment* **2018**, *190*, 716-721,https://doi.org/10.1007/s10661-018-7098-0.
17. Delgado, M.C.; García-Galvan, F.R.; Llorente, I.*et al*. Influence of aluminium enrichment in the near-surface region of commercial twin-roll cast AZ31 alloys on their corrosion behaviour. *Corros Sci.* **2017**, *123*, 182–196, https://doi.org/10.1016/j.corsci.2017.04.027.
18. Sanghvi, M.J.; Shukla, S.K.; Misra, A.N.; Padh, M.R.& Mehta, G.N. Evaluation of Abutilon indicum as Mild Steel Corrosion Inhibitor in 1 M HCl and 0.5 M H_2SO_4 by Electrochemical Techniques.*Asian Journal of Chemistry*,**2013**, *25*,1415-1419,http://dx.doi.org/10.14233/ajchem.2013.13045.
19. Xu, C.; Zhu, Y.; Liu, W. Hydrostatic pressure effects on corrosion behaviour of X80 steel in artificial sea water. *Corros Eng Sci Technol*. **2021**, *56*, 383–391, https://doi.org/10.1080/1478422X.2020.1866844.
20. Gupta, M.K.; Singhal, V. Review on materials for making lightweight vehicles. *Mater Today Proc*. **2022**, https://doi.org/10.1016/J.MATPR.2022.02.517.
21. Divya, P.; Subhashini, S.; Prithiba, A.; Rajalakshmi, R. An Evaluation of solid-state electrolyte based on Pectin and lithium bis (trifluoro methane sulphonyl) imide for Lithium-ion batteries.*Materials Today: Proceedings*, **2019**, *18*,1581–1591,https://doi.org/10.1016/j.matpr.2020.12.557.
22. Ramesh, S.P.; Vinodhkumar, K.P.;& Sethuraman, M.G. Seed Extract of Dypsis lutescens as Ecofriendly Corrosion Inhibitor for Mild Steel in Hydrochloric Acid Medium.*International Journal of ChemTech Research*, **2020 ,***13* , 149-158,http://dx.doi.org/10.20902/IJCTR.2019.130118.
23. Uo, S.W.; Xu, D.H. Corrosion characteristics and mechanisms of typical Ni-based corrosion-resistant alloys in sub- and supercritical water. *J Supercrit Fluids*. **2021**, *170*,https://doi.org/10.1016/j.supflu.2020.105138.
24. Liu, R.; Liu, L.; Wang, F. The role of hydrostatic pressure on the metal corrosion in simulated deep-sea environments – a review. *J Mater Sci Technol*.**2022**, *112*, 230–238, https://doi.org/10.1016/j.jmst.2021.10.014.
25. Shyamla,l C.; Rajesh, S.; Suresh, Kumar, S. A.Comprehensive review on the effect of precipitation on mechanical properties of friction stir welded aluminium alloys. *Proc Instit Mech Eng Pt C J Mech Eng Sci*. **2021**, *235*, 6345–6356, https://doi.org/10.1177/09544062211011519.
26. Matjaz Finsgar;& Jennifer Jackson. Application of corrosion inhibitors for steels in acidic media for the oil and gas industry A review. Corrosion Science **2014**, *86*, 17-41,http://dx.doi.org/10.1016/j.corsci.2014.04.044.
27. Wang, W.L.; He, L.; Yang, X. Microstructure and microhardness mechanism of selective laser melting Mg-Y-Sm-Zn-Zr alloy. *J Alloys Compd*. **2021**, *868*, 159107, https://doi.org/10.1016/j.jallcom.2021.159107.
28. Hao, J.; Zhang, J.; Li, B. Effects of 14H LPSO phase on the dynamic recrystallization and work hardening behaviors of an extruded Mg–Zn–Y–Mn alloy. *Mater Sci Eng A-Struct.* **2021**, *804*, 140727, https://doi.org/10.1016/j.msea.2020.140727.
29. Perumal, S.; Muthumanickam, S.; Elangovan, A.; Karthik, R.; Sayeekannan, R.;& Mothilal K.K. (Bauhinia tomentosa Leaves Extract as Green Corrosion Inhibitor for Mild Steel in 1M HCl Medium.*J Bio TriboCorros***2017**, *3*, 13-22,http://dx.doi.org/10.1007%2Fs40735-017-0072-5.

30. Akinbulumoa, O.A.; Johnson, O.; Odejobiab; Odekanleba, A.K.Thermodynamics and adsorption study of the corrosion inhibition of mild steel by Euphorbia heterophylla L. extract in 1.5 M HCl.*Results in Materials* **2020**, *5* ,100074-100079,https://doi.org/10.1016/j.rinma.2020.100074.
31. Lsa, B.; Ysa, C.; Kd, A. The change of cathode/anode roles and corrosion forms in 2024/Q235/304 tri-metallic couple with the variation of oxygen concentrations and area ratios. *Corros Sci*.**2021**, *184*, 19400, https://doi.org/10.1016/j.corsci.2021.109400.
32. Yuxin, W.; Bo, W.; Leyang, D.; ZHANG xianhui study on galvanic corrosion of low alloy steel in simulated marine low temperature environment. *J Chin Soc Corros Prot*. **2022**, *48*, 866–875, https://www.jcscp.org/EN/10.11902/1005.4537.2021.353.
33. Li, B.Z.; Zhang, Z.Q.; Qiu, Z.H. Insight to corrosion mechanism of 90/10 copper-nickel alloys under different sea depths. *Mater Lett.* **2021**, *15*, 130513, https://doi.org/10.1016/j.matlet.2021.130513.
34. Sha, B.; Rui, L.A.; Li, L.C. Influence of temperature and hydrostatic pressure on the galvanic corrosion between 90/10 Cu-Ni and AISI 316L stainless steel. *J Mater Res Technol*. **2021**;*13*, 1402–1415, https://doi.org/10.1016/j.jmrt.2021.05.067.
35. Olivares-Xometl, O.; Likhanova, A.V.; Martinez-Palou, R.;&Dominguez-Aguilar, M.A. Electrochemistry and XPS study of an imidazoline as corrosion inhibitor of mild steel in an acidic environment.*Materials and Corrosion* **2009**, *60*,14-21,https://doi.org/10.1002/maco.200805044.
36. E.EFoad El-SherbiniS; MAbd-El-Wahab ,M.A; Deyab. Studies on corrosion inhibition of aluminum in 1.0 M HCl and 1.0 M H_2SO_4 solutions by ethoxylated fatty acids.*Materials Chemistry and Physics***2003**, *82*, 631-637,https://doi.org/10.1016/S0254-0584(03)00336-5.
37. Agha Inya, N.;& Anyakwo, C.N. Modelling of Corrosion Inhibition of Mild Steel in Sulphuric Acid by thoroughly Crushed Leaves of Voacanga Africana. *American Journal of Engineering Research* **2017**, *6*, 344-356,http://www.ajer.org/.